THE JOURNAL OF BIOLOGICAL CHEMISTRY VOL. 285, NO. 49, pp. 38014–38022, December 3, 2010

Parathyroid Hormone Activation of Matrix Metalloproteinase-13 Transcription Requires the Histone Acetyltransferase Activity of p300 and PCAF and p300-dependent Acetylation of PCAF*

Received for publication, May 6, 2010, and in revised form, August 25, 2010 Published, JBC Papers in Press, September 24, 2010, DOI 10.1074/jbc.M110.142141

Minnkyong Lee[‡§] **and Nicola C. Partridge**[§1]

From the [‡]*Graduate School of Biomedical Sciences, University of Medicine and Dentistry of New Jersey, Piscataway, New Jersey 08854 and the* [§]*Department of Basic Science and Craniofacial Biology, New York University College of Dentistry, New York, New York 10010*

Parathyroid hormone (PTH) regulates the transcription of many genes involved in bone remodeling in osteoblasts. One of these genes is matrix metalloproteinase-13 (MMP-13), which is involved in bone remodeling and early stages of endochondral bone formation. We have previously shown that *Mmp-13* gene expression is highly induced by PTH treatment in osteoblastic UMR 106-01 cells, as well as primary osteoblasts. Here, we show that p300/CBP-associated factor (PCAF), in addition to p300 and Runx2, is required for PTH activation of *Mmp-13* transcription. PCAF was increasingly recruited to the MMP-13 proximal promoter region after PTH treatment, and this was associated with an increase in RNA polymerase II recruitment and histone acetylation. In addition, PTH treatment increased the acetylation of PCAF, a process that required p300. Knockdown of PCAF, p300, or Runx2 by siRNA decreased *Mmp-13* mRNA expression after PTH treatment in both UMR 106-01 cells and primary osteoblasts. We found that there is a mutual dependence between p300 and PCAF to be recruited to the *Mmp-13* promoter after PTH treatment. In promoter-reporter assays, p300 and PCAF had an additive effect on PTH stimulation of MMP-13 promoter activity, and this required their histone acetyltransferase activity. Our findings demonstrate that PCAF acts downstream of PTH signaling as a transcriptional coactivator that is required for PTH stimulation of MMP-13 transcription. PCAF cooperates with p300 and Runx2 to mediate PTH activation of *MMP-13* transcription.

PTH[2] is a peptide hormone that plays a central role in regulating serum ion concentrations. Secreted from the parathyroid glands in response to low serum calcium levels, PTH has two primary sites of action, bone and kidney. In bone, PTH stimulates the release of calcium and phosphate ions from the bone mineral matrix, leading to bone degradation such that PTH is classically known as a catabolic agent in bone remodeling. However, when administered intermittently, PTH has an anabolic effect that leads to increased bone mass. Binding of PTH to its receptor, PTH1R, on the surface of osteoblasts leads to the activation of many different signaling pathways, including protein kinase A (PKA)- and protein kinase C (PKC)-dependent pathways, as well as calcium ion channels (reviewed in Ref. 1). This eventually leads to a significant change in gene expression in osteoblasts (2). Microarray analyses from our laboratory demonstrated that the catabolic effect of PTH on bone predominantly occurs through PKA-dependent signaling (3).

MMP-13 is a collagenase that is expressed in chondrocytes, osteoblasts, and osteocytes. It plays an essential role in early stages of endochondral bone formation, and its expression is increased in pathological conditions such as osteoarthritis, rheumatoid arthritis, and tumor metastasis (4–6). *Mmp-13* gene expression is highly stimulated by PTH in osteoblastic UMR 106-01 cells (7), as well as *in vivo* (8). The relevance of MMP-13 and PTH has been demonstrated *in vivo* by the decreased expression of MMP-13 in *Pth1r* knock-out mice (9) and increased expression in rats treated with PTH (10). In addition, *Mmp-13*-null mice and PTH-null mice have similar phenotypes; both mice displayed elongated growth plates, extended hypertrophic chondrocyte regions, and delayed ossification (11–13).

Mutagenesis studies of the rat *Mmp-13* promoter have shown that the Runt domain (RD) and activator protein-1 (AP-1) site in the proximal promoter region are essential for PTH stimulation of *Mmp-13* promoter activity (14, 15). Runx2 binds to the RD sequence in promoter regions and regulates the expression of many bone-specific and bone-related genes, such as osteocalcin, osteopontin, and *MMP-13* (16–18). It is a critical transcription factor in osteoblast differentiation and maturation; mice with a homozygous mutation at the Runx2 locus are not viable and do not form bone due to a lack of mature osteoblasts (16, 19, 20). In addition, these mice do not express MMP-13, which demonstrates the regulatory role of Runx2 in the transcription of *Mmp-13* (21). Runx2 can function as a coactivator or corepressor of transcription depending on which factors it binds with at promoter regions. At the MMP-13 promoter in osteoblastic cells, we have shown that Runx2 binds HDAC4, resulting in a repression of transcription under basal conditions (22). After PTH treatment, HDAC4 dissociates from

* This work was supported, in whole or in part, by National Institutes of Health Grant DK47420 (to N. C. P.).

[1] To whom correspondence should be addressed. Tel.: 212-992-7145; Fax: 212-995-4204; E-mail: ncp234@nyu.edu.

[2] The abbreviations used are: PTH, parathyroid hormone; MMP-13, matrix metalloproteinase-13; HAT, histone acetyltransferases; PCAF, p300/CBP-associated factor; CBP, CREB-binding protein; CREB, cAMP-response element-binding protein; RNA pol II, RNA polymerase II.

Runx2, which is then free to recruit p300 to activate transcription (23).

The histone acetyltransferase p300 functions as a transcriptional coactivator through several different mechanisms. First, p300 is able to loosen the chromatin structure by directly acetylating histones via its intrinsic HAT activity, thus making the DNA more accessible to other transcriptional machinery (24, 25). In some cases, p300 acetylates non-histone proteins as well, such as p53 and Runx2, and regulates their transcriptional activity (26, 27). In other cases, the HAT activity of p300 is not necessary at all, and instead, it acts as a scaffold for binding additional transcription factors to promoter regions (18, 28). This mainly occurs through the CH1 and CH3 domains of p300, which are necessary for interacting with other transcription factors, such as c-Jun and PCAF (28, 29).

PCAF also has an intrinsic HAT domain and is able to acetylate nucleosomal and free H3 and H4 histones (30, 31). The HAT activity of PCAF is stimulated by the acetylation of lysine residues in the C terminus, which can occur via autoacetylation or by p300 but not by CBP (32). Before it was discovered that p300 and its functional homologue CBP had HAT activity, PCAF was considered to be the primary HAT involved in histone acetylation, whereas p300 and CBP were thought to act as adaptor molecules for PCAF and other transcription factors (24, 25).

Previous reports from our laboratory have shown that p300 associates with the MMP-13 proximal promoter through Runx2 after PTH treatment in UMR 106-01 cells and that both factors are necessary for PTH activation of MMP-13 transcription (23). Here, we report that PCAF is a downstream transcriptional coactivator of PTH that is required for *Mmp-13* transcription after PTH treatment in both UMR 106-01 cells and primary rat osteoblasts. In addition, PTH stimulation of *Mmp-13* promoter activity requires the HAT activity of both p300 and PCAF. These collectively suggest a model for PTH regulation of genes that have a Runt domain in their promoter region.

EXPERIMENTAL PROCEDURES

Antibodies and Reagents—Synthetic rat PTH-(1–34) was purchased from Sigma. Inhibitors H-89 and bisindolylmaleimide I were purchased from Calbiochem. Antibodies for PCAF (sc-8999), normal mouse IgG (sc-2025), and normal rabbit IgG (sc-2027) were purchased from Santa Cruz Biotechnology. Antibodies for p300 (05-257), acetyl-histone H3 (06-599), acetyl-histone H4 (06-598), and RNA pol II (05-623) were purchased from Millipore. Anti-acetylated lysine (9411) and anti-Runx2 (D130-3) were purchased from Cell Signaling and MBL International, respectively.

Plasmids—pGL2-MMP13, rat *Mmp-13* promoter region (−148/+14), was amplified using primers 5′-AAGGTACCACTCAGGTTCTGCCACA-3′ (forward) and 5′-AAGAGCTCCCTGGAGTCTCTCCTT-3′ (reverse) and then cloned into the KpnI and SacI sites of pGL2-basic vector (Promega). HA-PCAF was generated by subcloning the PCAF sequence from pcDNA3-PCAF-FLAG, kindly provided by Dr. Marian Martínez-Balbás (Instituto de Biología Molecular de Barcelona), into the HindIII and NotI sites of pHM6 vector (Roche Applied Science). HA-PCAF-A616/A617 was generated using the QuikChange multi site-directed mutagenesis kit (Stratagene). Residues 616 and 617 were substituted with alanine using primers 5′-GCAGATGAATATGCAATTGGAGCCGCTAAGAAACAGGGTTTCTCC-3′ (forward) and 5′-GGAGAAACCCTGTTTCTTAGCGGCTCCAATTGCATATTCATCTGC-3′ (reverse). Expression plasmids for p300, pCI-FLAG-p300 and pCI-FLAG-p300ΔHAT, were kindly provided by Dr. Yoshihiro Nakatani (Dana-Farber Cancer Institute, Harvard University) (28). All plasmids were sequenced and confirmed.

Cell Culture and Transient Transfection—UMR 106-01 cells were maintained in normal growth medium consisting of Eagle's minimal essential medium (1× non-essential amino acids, 1% penicillin-streptomycin) supplemented with 5% fetal bovine serum. For treatment with PTH or inhibitors, cells were grown to 80% confluency in normal growth medium and then subjected to serum starvation in minimal essential medium with 0.1% fetal bovine serum. For transfection, UMR 106-01 cells were seeded at a concentration of 1×10^5 cells/12 wells or 2×10^5 cells/6 wells 24 h prior to transfection. Plasmids were transfected using GeneJammer transfection reagent (Stratagene), and the amount of total DNA per well was normalized by adding pFLAG and pHM6 empty vectors. For siRNA transfection and cotransfection of siRNA and plasmids, X-tremeGENE siRNA transfection reagent (Roche Applied Science) was used according to the manufacturer's protocol. RNA oligoduplexes targeting rat p300 were purchased from Ambion and Sigma. RNA sequences targeting rat *Runx2* and PCAF were purchased from Sigma. Cells were collected 48 h after transfection for RNA analysis and 72 h after transfection for protein analysis and chromatin immunoprecipitation (ChIP) assays.

Rat Primary Calvarial Cell Isolation and Transient Transfection—Rat primary osteoblasts were isolated by the method of Shalhoub *et al.* (33). The cells were derived from postnatal day 1 rat calvariae by sequential digestions of 20, 40, and 90 min at 37 °C in 2 mg/ml collagenase A, 0.25% trypsin in Dulbecco's PBS solution. Cells from the first and second digests were discarded. Cells from the final digest were collected and plated at 2×10^5 cells/well in 6-well plates. The following day, cells were transfected with the indicated siRNA using X-tremeGENE siRNA transfection reagent at a final concentration of 100 nM. Cells were maintained in Eagle's minimal essential medium supplemented with 10% fetal bovine serum, non-essential amino acids, 1% penicillin-streptomycin for 48–72 h after transfection. Then, cells were treated with 10^{-8} M PTH-(1–34) for 2 h and collected for RNA analysis.

Luciferase Assay—Forty-eight hours after transfection, UMR 106-01 cells were treated with PTH-(1–34) for 6 h and collected in 1× Reporter Lysis Buffer (Promega). After at least 1 freeze-thaw cycle, luciferase activity of lysates was measured using the Dual-Luciferase reporter assay system (Promega) following the manufacturer's protocol. Luciferase activity was measured using the Optocomp™ II luminometer (MGM Instruments). Twenty μl of lysate was used per reading, and each sample was read in duplicate. Total firefly luciferase activity was normalized against total mg of protein used per sample.

TABLE 1
Primer sequences for real-time PCR

Gene	Primers (5′–3′)
Rat *Mmp-13* proximal promoter (−204/−34)	Forward, CAGATGCGTTTTGATATGCC Reverse, AATAGTGATGAGTCACCACTT
Rat *Mmp-13*	Forward, ACAGTTCAGGCTCAACCTGCTG Reverse, GCCCTATCCCTTGATGCCATT
Rat P*caf*	Forward, ATTCATGGCGGACTTACAGCGA Reverse, CTTGTCCATCAAGCCTGCTTCCTT
Rat *p300*	Forward, AGCGAGCTTATGCTGCTCTC Reverse, GGCACTCATGTTGTTCATGG
Rat *Runx2*	Forward, TAAAGTGACAGTGGACGGTCCC Reverse, TGCGCCCTAAATCACTGAGG
Rat c-*fos*	Forward, CTGCCTCTTCTCAATGACCCTG Reverse, GCCGGAAACAAGAAGTCATCAA
Rat β-actin	Forward, TCCTGAGCGCAAGTACTCTGTG Reverse, CGGACTCATCGTACTCCTGCTT

RNA Extraction and Real-time RT-PCR—UMR 106-01 cells were collected in Tri Reagent (Sigma), and RNA was subsequently isolated following the manufacturer's recommended protocol. RNA was subjected to reverse transcription using the TaqMan reverse transcription kit (Applied Biosystems), and the cDNA obtained was then amplified via real-time PCR using the SYBR Green PCR reagent (Applied Biosystems) with the indicated primers. Primer sequences used for real-time PCR are shown in Table 1. Real-time PCR data were normalized to β-actin, and -fold change in gene expression was obtained using the formula $2^{((\mathrm{Ctctrl} - \mathrm{Ct}\beta\text{-actin}) - (\mathrm{CtPTH} - \mathrm{Ct}\beta\text{-actin}))}$, where Ct is the threshold cycles and ctrl is the control.

Coimmunoprecipitation and Immunoblotting—UMR 106-01 cells were collected and lysed with radioimmunoprecipitation assay buffer (50 mM Tris-HCl, pH 7.4, 10 mM NaCl, 1 mM PMSF, 1 mM EDTA, 1% sodium deoxycholate, 0.1% SDS, and protease inhibitors) after the indicated treatments. Lysates were precleared with protein A/G-agarose beads (Santa Cruz Biotechnology) for 1 h at 4 °C, and the supernatants were then collected for overnight immunoprecipitation with the antibodies of interest. Normal rabbit or mouse IgG was used as a negative control depending on the origin of the antibody of interest. The next day, immunocomplexes were collected with protein A/G-agarose beads for 2 h at 4 °C and then washed three times with ice-cold PBS and resuspended in protein sample buffer.

Protein samples were resolved by SDS-PAGE and were transferred to polyvinylidene difluoride membranes. After blocking with 5% low fat milk in Tris-buffered saline (TBS) buffer containing 0.1% Tween 20, membranes were incubated overnight at 4 °C with primary antibodies in 5% low fat milk in TBS buffer. The following day, after washing, membranes were developed using enhanced chemiluminescence (Amersham Biosciences). All Western blots were quantified through densitometry using ImageQuant 5.0 software.

ChIP Assay—UMR 106-01 cells were grown to confluency and treated with 10^{-8} M PTH-(1–34) for 30 min, 1 h, or 2 h and subsequently incubated in 1% formaldehyde for 15 min. Cells were then collected in SDS-lysis buffer and sonicated on ice with four 10-s pulses with 20-s intervals. Following centrifugation for 10 min at 14,000 × g, the supernatants were collected and diluted with ChIP dilution buffer. After preclearing with protein G-agarose beads/salmon sperm DNA, the supernatants were collected for overnight incubation at 4 °C with the antibodies of interest. The following day, immunocomplexes were collected with protein G-agarose beads/salmon sperm DNA for 2 h at 4 °C and were subsequently washed with the following: once with low salt washing buffer, high salt washing buffer, LiCl washing buffer and twice with Tris-EDTA buffer. To elute DNA, samples were incubated twice in 150 μl of elution buffer (1% SDS and 0.1 M $NaHCO_3$) for a total of 30 min at room temperature. The supernatant from each elution was collected and incubated at 65 °C for at least 5 h to reverse cross-linking after the addition of 12 μl of 5 M NaCl. The next day, following treatment with RNase A and proteinase K, DNA was purified by phenol-chloroform extraction. DNA was then amplified using real-time PCR using the primers for the rat *Mmp-13* proximal promoter region (−204/−34) (Table 1). The data obtained were analyzed using the formula $2^{((\mathrm{CtIgG} - \mathrm{Ct\ Input}) - (\mathrm{CtAb} - \mathrm{CtInput}))}$, where Ct is the threshold cycles, IgG is the normal IgG, Ab is the specific antibody, and Input is the input genomic DNA (34).

Statistical Analysis—Data are shown as the average ± S.E. of at least three independent experiments. For luciferase assays and RNA analyses, each independent experiment was performed in triplicate, and each sample was measured in duplicate. Statistical significance was assessed using Student's *t* test.

RESULTS

PCAF Is Recruited to the MMP-13 Proximal Promoter Region with PTH Treatment—Previous work from our laboratory has shown that p300 is recruited to the *Mmp-13* proximal promoter region after PTH treatment in osteoblastic UMR 106-01 cells (23). Although the HAT activity of p300-immunoprecipitated complexes increased with PTH treatment (23), we were not able to identify a change in post-translational modification in p300 that could explain the increase in HAT activity (data not shown). In the process of identifying another candidate that could be responsible for the increase in HAT activity, we found that PCAF, another well defined HAT, coimmunoprecipitated with p300 in UMR 106-01 cells with and without PTH treatment (Fig. 1*A*). PCAF is an acetylated protein, and acetylation of PCAF has been reported to augment its HAT activity (32). We found that after 1 h of PTH treatment, PCAF acetylation increased 50% in UMR 106-01 cells (Fig. 1*B*). To determine whether PCAF is involved in the transcriptional regulation of *Mmp-13*, we performed ChIP assays using UMR 106-01 cells treated with PTH for 30 min, 1 h, or 2 h (Fig. 1*C*). ChIP DNA samples were amplified using primers for the proximal promoter region of *Mmp-13* (−204/−34). Results from these experiments demonstrate that recruitment of PCAF and p300 to the *Mmp-13* promoter increases with PTH treatment when compared with control sets, and this is associated with an increase in histone acetylation and a significant increase in *Mmp-13* mRNA (Fig. 1*D*). Inhibition of PKA signaling by 5 μM H-89 completely blocked the binding of p300, PCAF, and RNA pol II after 2 h of PTH treatment. The binding of RNA pol II, which we used in ChIP assays as a positive control for active promoters, was somewhat affected by the inhibition of PKC by 5 μM bisindolylmaleimide-1 (Fig. 1*E*). However, this decrease was statistically insignificant, most likely due to the large degree of variation in the -fold change of RNA pol II. This may be

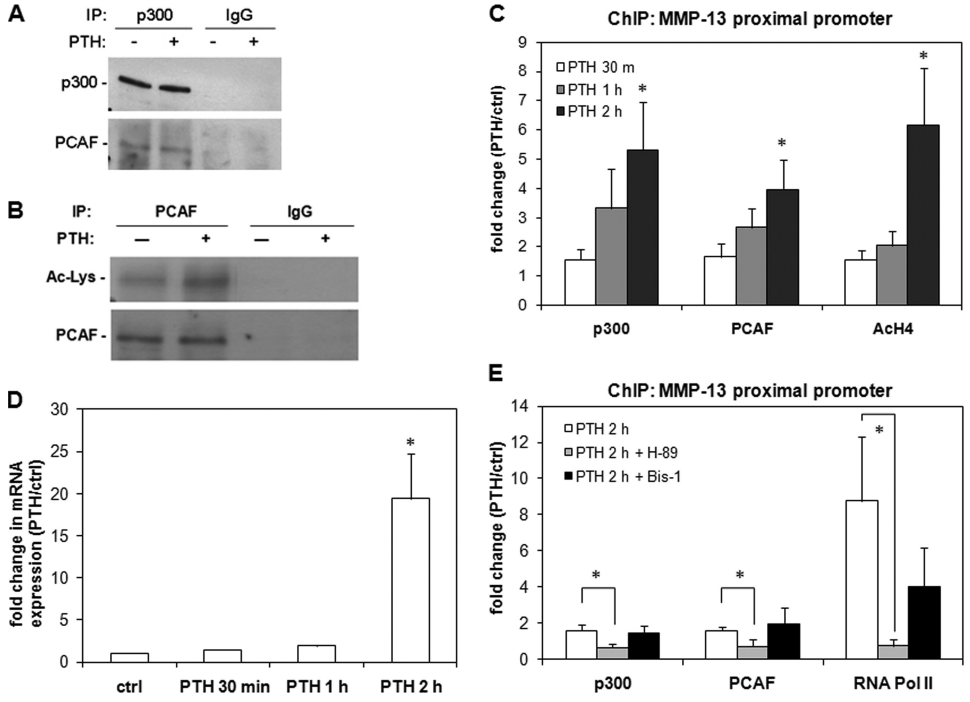

FIGURE 1. **PTH stimulates the recruitment of p300 and PCAF to the proximal promoter region of *Mmp-13* through PKA signaling pathways and causes acetylation of PCAF.** *A*, association of p300 and PCAF in PTH-treated osteoblastic cells. UMR 106-01 cells were treated with or without 10^{-8} M PTH for 1 h, and lysates were collected for overnight immunoprecipitation (*IP*) with anti-p300 or normal mouse IgG. Protein samples were resolved using 6% SDS-PAGE and then subjected to immunoblotting with p300 or PCAF antibodies. *B*, PTH causes increased acetylation of PCAF in osteoblastic cells. UMR 106-01 cells were treated with or without PTH for 1 h, and then lysates were collected for overnight immunoprecipitation with anti-PCAF or normal rabbit IgG. Protein samples were resolved using 6% SDS-PAGE and then subjected to immunoblotting with antibodies against acetylated lysine or PCAF. Data shown are representative of three independent experiments. Western blots were quantified through densitometry using the ImageQuant 5.0 software, and acetylation was normalized to the amount of total PCAF. *ctrl*, control. *C*, PTH causes recruitment of p300 and PCAF to the *Mmp-13* promoter. ChIP assays were performed with UMR 106-01 cells collected after the indicated time points. DNA was amplified via real-time PCR using primers for the *Mmp-13* promoter (−204/−34). Data are shown as -fold change to control after normalizing to input and IgG (34). *, $p < 0.05$ when compared with control. *D*, PTH stimulation of *Mmp-13* mRNA. Total RNA was isolated from UMR 106-01 cells after treatment with PTH for the indicated time points. Expression of *Mmp-13* mRNA was determined via real-time RT-PCR. *, $p < 0.05$ when compared with control. *E*, PTH regulates recruitment of p300 and PCAF to the *Mmp-13* promoter through the PKA pathway. ChIP assays were performed with UMR 106-01 cells treated with dimethyl sulfoxide (DMSO) (control), 5 μM H-89 (PKA inhibitor), or 5 μM bisindolylmaleimide I (*Bis-1*; PKC inhibitor) for 40 min prior to 2 h of PTH treatment. Data are shown as -fold change to control. *, $p < 0.05$ between the indicated sets. *Error bars* represent ± S.E. of at least three independent experiments.

because the amount of pol II associated with the promoter changes rapidly and highly with time, thus giving greater variation from one experiment to the next.

PCAF Is Required for PTH-dependent p300 Recruitment and Transcriptional Activation of MMP-13—PCAF acts as a transcriptional coactivator for many genes (18, 35, 36), although it has not yet been reported to be involved downstream of PTH signaling or in *MMP-13* transcription. To determine whether PCAF plays a critical role in the PTH activation of *Mmp-13* transcription, PCAF expression was transiently knocked down in UMR 106-01 cells via siRNA transfection. Knockdown of PCAF was confirmed at both the RNA and the protein level; an average of 45% knockdown in PCAF mRNA (Fig. 2*A*) and an average of 90% knockdown in protein expression (Fig. 2*B*) were observed. In whole cell lysates, the PCAF antibody detects two additional bands. These may be different isoforms of PCAF that are expressed in rat. However, these additional bands are not detected after immunoprecipitation (Fig. 1*B*). Analysis of RNA collected from these cells shows that targeting of PCAF siRNA is specific, demonstrated by the mRNA expression of *p300* (Fig. 2*A*), which was not affected by the transfection of PCAF siRNA.

In cells transfected with PCAF siRNA, the increase in *Mmp-13* mRNA in response to PTH was diminished by 70% when compared with those cells transfected with scrambled siRNA (Fig. 2*A*), confirming that PCAF is necessary for PTH-dependent *MMP-13* transcription. The expression of c-*fos*, another PTH-responsive gene, was not affected, which indicates that this requirement for PCAF does not apply to all genes that are regulated by PTH. We next performed ChIP assays with PCAF siRNA-transfected cells to examine the role of PCAF in p300 recruitment and histone acetylation at the *Mmp-13* promoter. Surprisingly, knockdown of PCAF resulted in the abolition of p300 recruitment (Fig. 2*C*), implying that PCAF is required for p300 association with the *MMP-13* promoter. In addition, recruitment of transcriptional machinery such as RNA pol II and histone acetylation decreased as well, which accounts for the decrease in *Mmp-13* transcription.

Recruitment of PCAF to the MMP-13 Proximal Promoter Requires Runx2—We have previously shown that p300 association with the *Mmp-13* proximal promoter requires Runx2 (23). Because PCAF was found to coimmunoprecipitate with p300, we examined whether PCAF was also binding to the *Mmp-13* promoter through Runx2 in a similar manner. Using siRNA, the expression of Runx2 was knocked down an average of 51% at the mRNA level and 40% at the protein level in UMR 106-01 cells (Fig. 3, *A* and *B*). RNA analysis showed that cells with a significant knockdown of *Runx2* mRNA had an 86% decrease in *Mmp-13* transcription after 2 h of PTH treatment (Fig. 3*C*). We also performed ChIP assays using cells transfected with *Runx2* siRNA. Results from these experiments demonstrate that cells expressing less Runx2 were not able to recruit PCAF or p300 to the *Mmp-13* proximal promoter after 2 h of PTH treatment (Fig. 3*C*). Knockdown of Runx2 expression also abolished the increase in RNA pol II association and histone acetylation when compared with that of cells transfected with scrambled siRNA. The decrease observed in RNA pol II association was outside of the statistically significant range, most likely due to the greater degree of variability in the -fold change of RNA pol II.

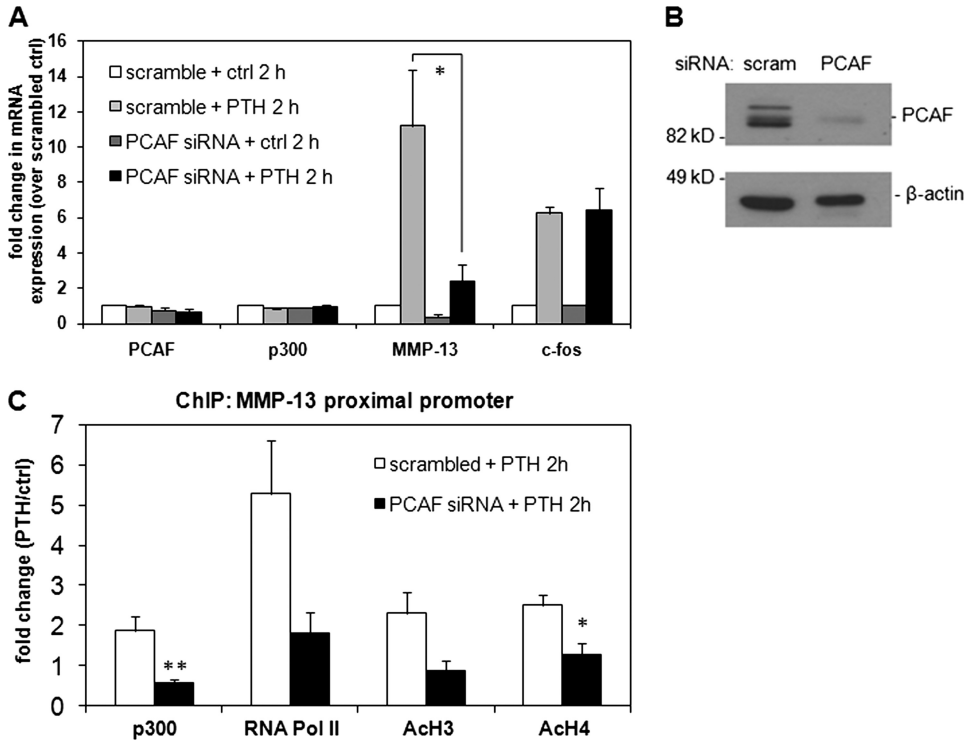

FIGURE 2. **Knockdown of PCAF abolishes PTH activation of *Mmp-13* transcription.** UMR 106-01 cells were transfected with 50 nM PCAF siRNA or scrambled siRNA. *A*, mRNA expression after PCAF knockdown. Forty-eight hours after transfection, cells were treated with 10^{-8} M PTH-(1–34) for 2 h and collected for RNA analysis. Total RNA was isolated and amplified via real-time RT-PCR. Relative levels of mRNA were normalized to β-actin. Data are shown as -fold change to scrambled control (*ctrl*). *Error bars* represent ± S.E. of three independent experiments. *, $p < 0.05$ between the indicated sets. *B*, Western blot of PCAF. Seventy-two hours after transfection, whole cell lysates were collected for protein expression analysis. Protein samples were separated using 6% SDS-PAGE and immunoblotted with antibodies against PCAF and β-actin as indicated. *scram*, scrambled siRNA. *C*, knockdown of PCAF decreases recruitment of p300 and acetylation at the *Mmp-13* promoter. Seventy-two hours after transfection, cells were treated with 10^{-8} M PTH-(1–34) for 2 h and collected for ChIP assays with antibodies against p300, RNA pol II, AcH3, AcH4, or IgG as a negative control. DNA was amplified by real-time PCR using primers for rat *Mmp-13* proximal promoter region (−204/−34). Data are shown as -fold change to each control. *Error bars* represent ± S.E. of at least three independent experiments. * and ** indicate $p < 0.05$ and $p < 0.001$ when compared with PTH-treated scrambled set, respectively.

p300 Is Necessary for PCAF Association with the MMP-13 Proximal Promoter and PCAF Acetylation—Results from the PCAF siRNA ChIP assays seemed to suggest a dependence on PCAF for the recruitment of p300 (Fig. 2*C*). To determine whether p300 is also necessary for PTH-dependent recruitment of PCAF to the *Mmp-13* promoter, we knocked down the expression of p300 using siRNA in UMR 106-01 cells. ChIP assay results from cells transfected with *p300* siRNA or scrambled siRNA demonstrate that binding of PCAF and RNA pol II to the *Mmp-13* promoter region requires p300 (Fig. 4*A*). In previous studies, the HAT activity of p300 has been shown to acetylate PCAF, which augmented its HAT activity (32). In UMR 106-01 cells, with the knockdown of p300, there was no increase in PCAF acetylation after PTH treatment when compared with the 2-fold increase observed in cells transfected with scrambled siRNA, demonstrating that p300 is required for PTH-dependent acetylation of PCAF (Fig. 4*B*). This was associated with a 33% decrease in *Mmp-13* mRNA after 2 h of PTH treatment when compared with scrambled siRNA samples (Fig. 4*C*). In PTH-treated samples, a decrease in *Runx2* mRNA levels was observed after knockdown of p300. It is possible that p300 plays a role in the up-regulation of Runx2 expression with PTH treatment; however, this has not yet been confirmed, and the slight decrease we observed was statistically insignificant. We confirmed the knockdown of p300 expression at the mRNA and protein level via real-time RT-PCR and Western blot analysis (Fig. 4, *C* and *D*).

PTH Response of MMP-13 Transcription Requires the Cooperation of PCAF, p300, and Runx2 in Primary Rat Osteoblasts—UMR 106-01 cells have certain osteoblastic phenotypes that make them useful models for studying PTH signaling. However, we realize that because they are derived from a rat osteosarcoma, there are differences that distinguish them from non-cancerous cells. To examine whether the dependence upon PCAF, p300, and Runx2 for *MMP-13* transcription is a generalized osteoblast event, we repeated the knockdown of each factor in rat primary calvarial osteoblasts. A 33% knockdown of PCAF mRNA was achieved, and this caused a 49% decrease in *Mmp-13* transcription after 2 h of PTH treatment (Fig. 5*A*). A 29% knockdown of *p300* mRNA led to a 32% decrease in *Mmp-13* transcription after 2 h of PTH treatment (Fig. 5*B*). A 43% knockdown in *Runx2* mRNA resulted in a 61% reduction in *Mmp-13* mRNA transcription after PTH stimulation (Fig. 5*C*). These results confirm that PTH activation of *Mmp-13* transcription in primary osteoblastic cells also requires PCAF, p300, and Runx2. In addition, similar to the results seen in UMR 106-01 cells, the most significant effect was seen with the knockdown of Runx2, suggesting that Runx2 is a crucial factor in the recruitment of p300 and PCAF, and activation of *MMP-13* transcription.

Functional Cooperation of p300 and PCAF in the PTH-dependent Activation of the MMP-13 Promoter—Cooperation between p300 and PCAF has been reported in various cases, although it seems that they have distinct roles rather than complementary functions as HATs (18, 26, 36–38). Based on our ChIP assay results using siRNA, we determined that there was a mutual dependence between p300 and PCAF for full activation of *MMP-13* transcription. We further tested this by performing promoter-reporter assays in which the expression of the firefly luciferase gene was controlled by the rat *Mmp-13* promoter (−148/+14). PTH treatment of UMR cells stimulated the *Mmp-13* promoter activity, and the addition of either p300 or PCAF further enhanced the PTH response (Fig. 6*A*, *lanes 1*-3). However, the highest level of stimulation was achieved only with the addition of both p300 and PCAF (Fig. 6*A*, *lane 6*).

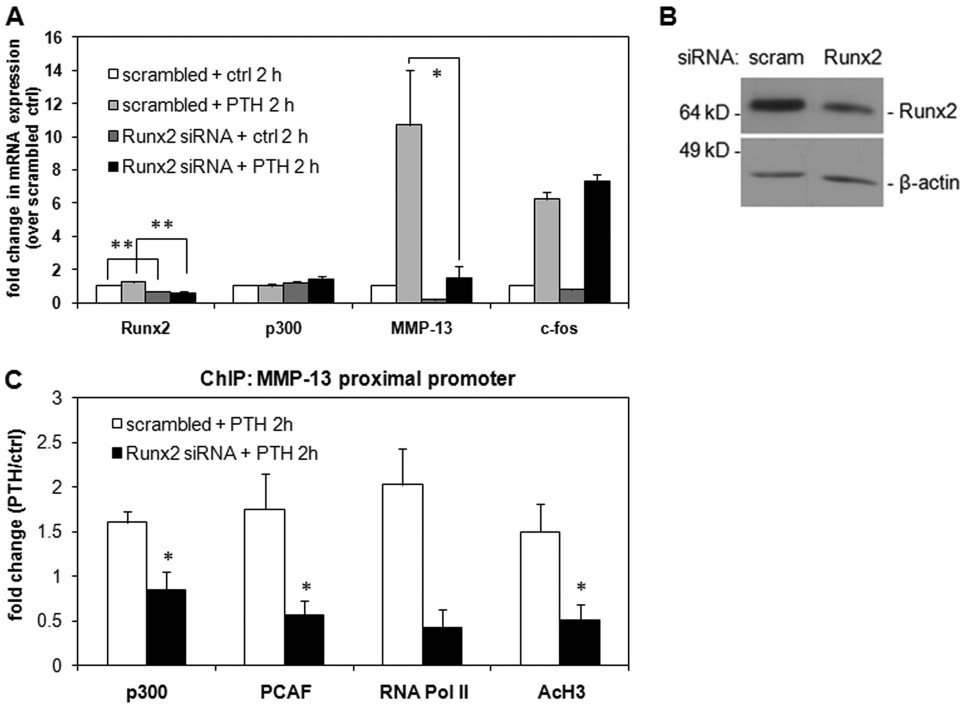

FIGURE 3. **Knockdown of *Runx2* represses PTH-dependent recruitment of PCAF and subsequent *Mmp-13* transcription.** UMR 106-01 cells were transfected with 50 nM Runx2 siRNA or scrambled siRNA. *A*, mRNA expression after *Runx2* knockdown. Forty-two hours after transfection, cells were treated with 10^{-8} M PTH-(1–34) for 2 h and collected for RNA analysis. Total RNA was isolated and amplified via real-time RT-PCR. Relative levels of mRNA were normalized to β-actin. Data are shown as -fold change to scrambled control (*ctrl*). *Error bars* represent ± S.E. of at least three independent experiments. * and ** indicate $p < 0.05$ and $p < 0.005$ between the indicated sets, respectively. *B*, Western blot of Runx2. Seventy-two hours after transfection, whole cell lysates were collected for protein expression analysis. Samples were separated using 8% SDS-PAGE and immunoblotted with antibodies against Runx2 and β-actin as indicated. Quantitation was performed using the ImageQuant 5.0 software. *C*, knockdown of *Runx2* decreases recruitment of p300 and PCAF and acetylation at the *Mmp-13* promoter. Seventy-two hours after transfection, cells were treated with 10^{-8} M PTH-(1–34) for 2 h and collected for ChIP assays with antibodies against p300, PCAF, RNA pol II, AcH3, or IgG as a negative control. DNA was amplified by real-time PCR using primers for rat *Mmp-13* proximal promoter region (−204/−34). *Error bars* represent ± S.E. of at least three independent experiments. *, $p \leq 0.05$ when compared with PTH-treated scrambled set.

We reasoned that the increase in promoter activity seen with the addition of only one of p300 or PCAF was due to the presence of endogenous PCAF or p300, respectively. To examine whether this was true, we knocked down the expression of endogenous *p300* or PCAF using siRNA in UMR 106-01 cells and cotransfected p300 and PCAF plasmids as indicated (Fig. 6*B*). Because the siRNA was designed against rat *p300* or PCAF and the plasmids for p300 and PCAF were made using human genes, the siRNA did not affect the expression of the exogenous plasmids (data not shown). With the knockdown of *p300* or PCAF, the addition of either enzyme alone did not augment the promoter activity of MMP-13 as it had done previously (Fig. 6*B*, *lanes 5* and *7*). Only when the knockdown was rescued by the addition of exogenous *p300* or PCAF (Fig. 6*B*, *lanes 6* and *8*) was the PTH stimulation of *MMP-13* promoter activity enhanced close to levels observed before.

Although the intrinsic HAT activity of both p300 and PCAF is known to be central to their role as transcriptional coactivators, the necessity of the HAT activity of each factor seems to vary from case to case. For instance, the activation of the osteocalcin promoter by 1,25-$(OH)_2$ vitamin D_3 does not require the HAT activity of p300, although the presence of p300 increased osteocalcin promoter activity (18). In a different case regarding the *COX-2* gene, HAT activity of p300 was essential for transcriptional activation (36). To determine the situation for the PTH stimulation of the *MMP-13* promoter, we substituted wild-type p300 and PCAF plasmids with mutant constructs, pCI-FLAG-p300ΔHAT and HA-PCAF-A616/A617, which were previously shown to not have intrinsic HAT activity (28, 39). Amino acids (1603–1653) in the HAT domain were deleted from the wild-type p300 construct and ligated to make pCI-FLAG-p300ΔHAT. HA-PCAF-A616/A617 was made by mutating residues 616 and 617 in the co-enzyme A binding domain that were shown to be important for intrinsic HAT activity (39). In promoter-reporter assays of *Mmp-13*, the addition of either HAT mutant construct did not have the stimulatory effect previously observed with the addition of wild-type p300 or PCAF (Fig. 6*A*, *lanes 4* and *5*). The addition of HA-PCAF-A616/A617 and p300 or pCI-FLAG-p300ΔHAT and PCAF (Fig. 6*A*, *lanes 7* and *8*) did not enhance the *Mmp-13* promoter activity as much as when wild-type p300 and PCAF were coexpressed. Taken together, these results suggest that PTH activation of *Mmp-13* promoter activity requires the HAT activity of both p300 and PCAF for full stimulation after PTH treatment.

DISCUSSION

PTH regulates the expression of many different genes in osteoblasts, yet the underlying molecular mechanism is not yet fully understood. Our previous results demonstrated p300 to be an essential HAT in the PTH-dependent transcriptional activation of *Mmp-13*, where the HAT activity of p300, but not that of CBP, increased with PTH treatment (23). However, we were not able to identify any post-translational modifications that could explain the increase in HAT activity seen in the p300-immunoprecipitated complexes. Here, we identified another HAT, PCAF, to be involved downstream of PTH signaling in the transcriptional activation of *Mmp-13* in osteoblastic UMR 106-01 cells. PCAF is an acetylated protein, and sequence analysis of human PCAF identified over 30 putative acetylation sites on internal lysines (determined by PAIL (prediction of *N*ϵ-acetylation on internal lysines) (40), an online program for predicting acetylation of internal lysines, data not shown), and increased acetylation has been reported to enhance its intrinsic HAT activity (32). We found that PCAF coimmunoprecipitates with p300 in UMR 106-01 lysates (Fig. 1*A*), and its acetylation is

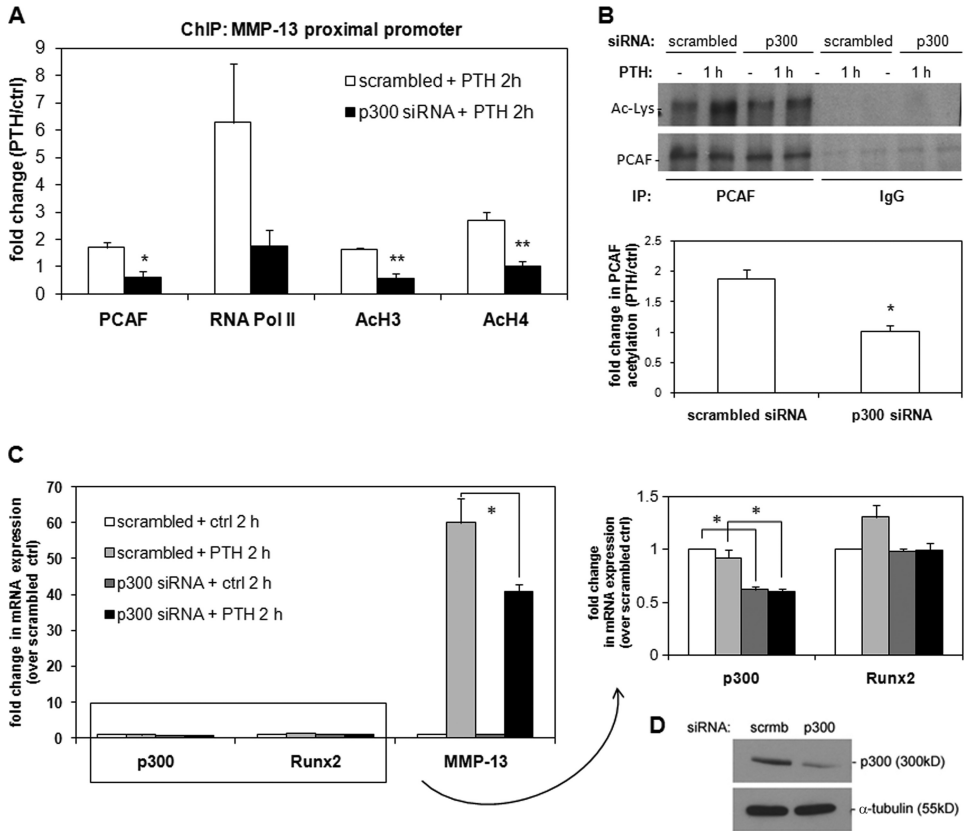

FIGURE 4. **Recruitment of PCAF and its acetylation after PTH treatment and subsequent *Mmp-13* transcription decrease with knockdown of *p300*.** UMR 106-01 cells were transfected with 50 nM *p300* siRNA or scrambled siRNA. *A*, recruitment of PCAF and histone acetylation at the *Mmp-13* promoter is decreased by *p300* knockdown. Seventy-two hours after transfection, cells were treated with 10^{-8} M PTH-(1–34) for 2 h and collected for ChIP assays with antibodies against PCAF, RNA pol II, AcH3, AcH4, or IgG as a negative control (*ctrl*). DNA was amplified by real-time PCR using primers for the rat *Mmp-13* proximal promoter region (−204/−34). *Error bars* represent ± S.E. of three independent experiments. * and ** indicate $p < 0.05$ and $p < 0.005$ when compared with scrambled set, respectively. *B*, PTH-dependent acetylation of PCAF requires p300. UMR 106-01 cells were transfected with 50 nM *p300* siRNA or scrambled siRNA and collected 72 h after transfection for immunoprecipitation (*IP*) with anti-PCAF or normal rabbit IgG after 1 h of PTH treatment. Protein samples were resolved using 6% SDS-PAGE and immunoblotted with antibodies against acetylated lysine or PCAF. Quantitation was performed using the ImageQuant 5.0 software, and acetylation was normalized to the amount of total PCAF. *Error bars* represent ± S.E. of three independent experiments. *, $p < 0.01$ when compared with PTH-treated scrambled set. *C*, mRNA expression after *p300* knockdown. Forty-eight hours after transfection, cells were treated with 10^{-8} M PTH-(1–34) for 2 h and collected for RNA analysis. Total RNA was isolated and amplified via real-time RT-PCR. Relative levels of mRNA were normalized to β-actin. Data are shown as -fold change to scrambled control. *Error bars* represent ± S.E. of three independent experiments. *, $p \leq 0.05$ between the indicated sets. *D*, Western blot for p300. Seventy-two hours after transfection, whole cell lysates were collected for protein expression analysis. Protein samples were separated using 6% SDS-PAGE and immunoblotted with antibodies against p300 and α-tubulin as indicated. *scrmb*, scrambled siRNA.

increased with 1 h of PTH treatment (Fig. 1*B*), which suggests that PCAF may be responsible for the increase in HAT activity in p300 immunocomplexes after PTH treatment.

Our results here demonstrate that PCAF is required for the full transcriptional activation of *MMP-13* in response to PTH treatment. In both UMR 106-01 cells and rat primary osteoblasts, knockdown of PCAF via siRNA caused a decrease in *Mmp-13* transcriptional activation after 2 h of PTH treatment (Fig. 2, *A* and *C*). In both cell types, the highest level of knockdown was achieved with Runx2, which resulted in the most significant decrease in *Mmp-13* transcription when compared with knockdown of *p300* or PCAF (Fig. 3*A*). A reason for this observation may be that Runx2 directly binds to the *MMP-13* promoter and may be responsible for recruiting other transcriptional coactivators, in addition to p300 and PCAF. In comparison, although they are still critical for *MMP-13* transcription, p300 and PCAF seem to play a lesser role in recruiting other coactivators, resulting in the smaller knockdown of *Mmp-13* transcription (Figs. 2*A* and 4*A*).

PTH can activate multiple signaling pathways in osteoblasts, although it seems to be predominantly dependent on PKA. Gene expression studies in rats treated with different PTH peptides have shown that PTH-(1–31), which selectively activates the PKA pathway and calcium ion signaling, has closely similar effects to that of the full-length synthetic peptide PTH-(1–34) (3). PTH-(3–34), which only activates calcium ion signaling and the PKC pathway, regulated very few genes, demonstrating the limited role of PKC and likely the intracellular calcium pathway in PTH signaling in osteoblasts. Accordingly, PTH regulation of *Mmp-13* is mainly mediated through PKA (7, 41). Inhibition of PKA abolishes PTH activation of *Mmp-13* promoter activity and sequential transcription (41). Our results shown here suggest that one reason is due to the lack of p300 and PCAF at the promoter region after PTH treatment.

Interestingly, recruitment of RNA pol II, but not that of p300 or PCAF, was affected by the inhibition of PKC signaling. This suggests the possibility that activation or recruitment of RNA pol II by PTH requires PKC signaling and that binding of p300 and PCAF at the *MMP-13* promoter region is not sufficient for RNA pol II association. Because RNA pol II phosphorylation is crucial for its activity and because its C-terminal repeat domain is heavily phosphorylated, it is possible that a kinase activated downstream of PKC regulates the binding of RNA pol II. However, the decrease observed in RNA pol II association was determined to be statistically insignificant, and PKC inhibition by bisindolylmaleimide I does not have an effect on PTH stimulation of *Mmp-13* transcription in UMR 106-01 cells. Thus, even if RNA pol II binding is partly dependent on PKC signaling, it is minimal because the activation by PKA alone is sufficient to generate *MMP-13* mRNA transcripts in response to PTH treatment.

Knockdown of PCAF abolishes the PTH stimulation of p300 recruitment to the *Mmp-13* promoter (Fig. 2*C*). There seems to

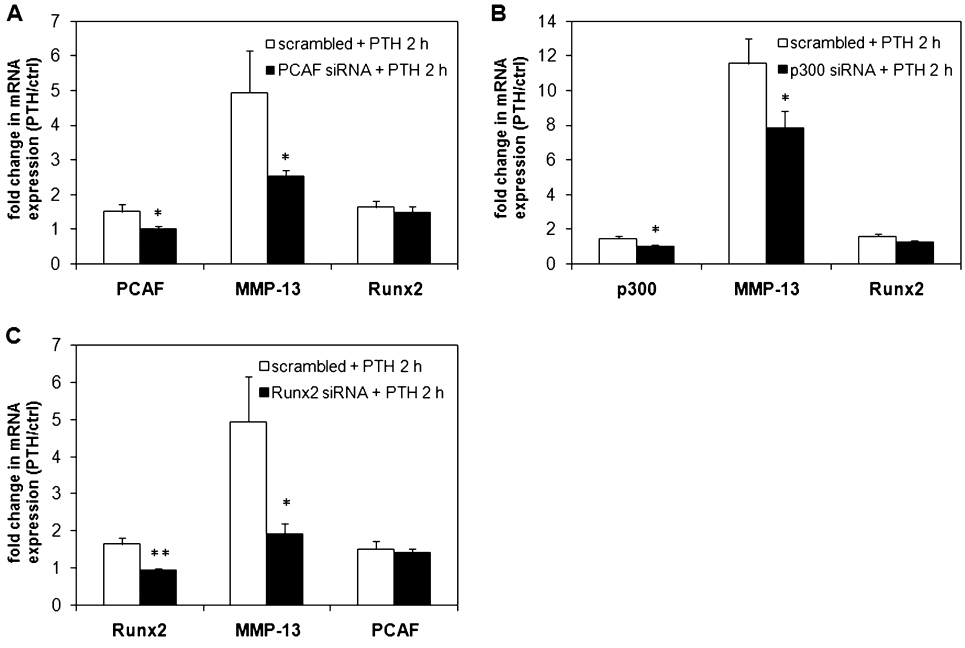

FIGURE 5. **Inhibition of PCAF, *p300*, or *Runx2* expression in primary rat osteoblastic cells decreases PTH-dependent *Mmp-13* transcription.** *A–C*, primary osteoblasts were isolated from 1-day-old rat pup calvariae and plated at 2×10^5 cells/well in 6-well plates. The next day, cells were transfected with PCAF, p300, Runx2, or scrambled siRNA as indicated. Between 48 and 72 h after transfection, cells were treated with 10^{-8} M PTH-(1–34) for 2 h and collected for RNA isolation. Relative levels of mRNA were normalized to β-actin. Data are shown as -fold change to scrambled control (*ctrl*). *Error bars* represent ± S.E. of at least three independent experiments. * and ** indicate $p \leq 0.05$ and $p < 0.005$ when compared with PTH-treated scrambled set, respectively.

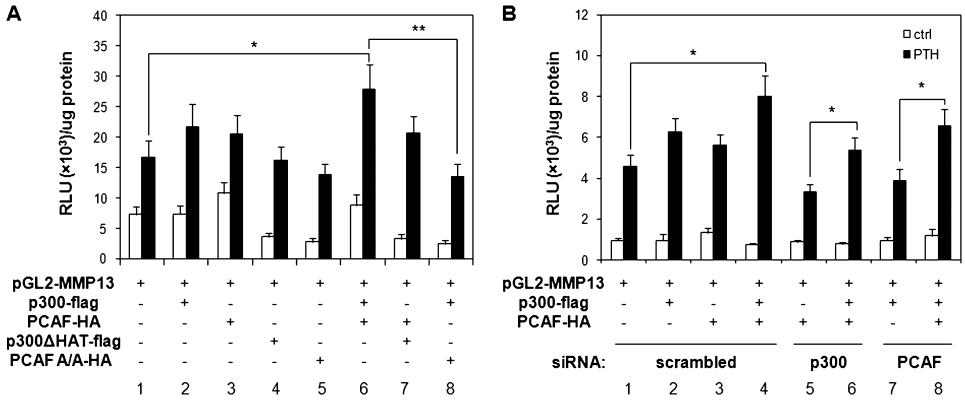

FIGURE 6. **Both PCAF and p300 and their HAT activities are required to stimulate *Mmp-13* promoter activity.** *A*, UMR 106-01 cells were plated in 12-well plates and transfected with 100 ng of pGL2-MMP13 and 150 ng of p300 and PCAF constructs as indicated. Firefly luciferase activity was measured after 6 h of PTH treatment, and relative light units (*RLU*) were normalized to the amount of total protein (μg) per sample. *Error bars* represent ± S.E. of three independent experiments. * and ** indicate $p < 0.05$ and $p \leq 0.006$ between the indicated sets, respectively. *B*, UMR 106-01 cells were plated in 12-well plates. pGL2-MMP13, p300, and PCAF plasmids were cotransfected with 50 nM scrambled, *p300*, or PCAF siRNA as indicated. Firefly luciferase activity was measured after 6 h of PTH treatment and normalized to the total protein amount (μg) per sample. *Error bars* represent ± S.E. of three independent experiments. * and ** indicate $p < 0.05$ and $p \leq 0.006$ between the indicated sets, respectively.

binding of p300/CBP. We suggest that in the absence of nuclear receptors, as is the case for PTH signaling, cells use a different regulatory system that requires PCAF and p300 to interact with each other to bind to promoters.

Previous studies have reported different requirements for the HAT activity of p300 and PCAF. In the activation of the osteocalcin promoter by vitamin D_3 in osteoblastic cells, Sierra *et al.* (18) demonstrated that although p300 and PCAF have additive effects on the osteocalcin promoter, the intrinsic HAT activity of p300 is dispensable. Similarly, for muscle cell differentiation and survival, the HAT activity of PCAF was required, but not that of p300 (28, 43). In contrast, the HAT activity of p300 was essential for *COX-2* gene transcription (36) and Notch intracellular domain signaling (37). As demonstrated by our results shown here, for the PTH activation of *MMP-13* transcription, the HAT activity of both p300 and PCAF seem to be necessary (Fig. 6*A*). It is interesting that the enzymatic activity of PCAF is critical for many physiological processes, yet mice lacking PCAF are viable and have a generally normal phenotype (44, 45). In contrast, mice with a deletion in p300 are embryonic lethal (46). The different phenotypes of these mice demonstrate that p300 and PCAF are not interchangeable and play significantly different roles during different stages of development. We hypothesize that this applies to the PTH activation of *MMP-13* transcription, in which the functional role of each HAT is different; our data suggest that p300 may play a role in stimulating PCAF, most likely via acetylation, whereas PCAF plays a central role at the promoter region in histone acetylation.

be a mutual dependence between PCAF and p300 because the knockdown of p300 abolishes the recruitment of PCAF as well (Fig. 4*C*). This suggests a regulatory mechanism in which PCAF and p300 are required to form a complex prior to binding to the promoter after PTH treatment. This is different from the report of Blanco *et al.* (42), in which the interaction of PCAF and p300 with the retinoid X receptor-retinoic acid receptor heterodimer is independent of each other. They suggested that PCAF first binds directly with receptors that are bound to DNA, which is then followed by

Acknowledgments—We thank Drs. Jeong Hoon Kim (University of Southern California) and Marian Martínez-Balbás (Instituto de Biología Molecular de Barcelona) for providing p300 and PCAF expression plasmids and Drs. Marc Gartenberg, Chih-Cheng Tsai, and Emi Shimizu for helpful discussions.

REFERENCES

1. Lee, M., and Partridge, N. C. (2009) *Curr. Opin. Nephrol. Hypertens.* **18,** 298–302
2. Qin, L., Qiu, P., Wang, L., Li, X., Swarthout, J. T., Soteropoulos, P., Tolias, P., and Partridge, N. C. (2003) *J. Biol. Chem.* **278,** 19723–19731
3. Li, X., Liu, H., Qin, L., Tamasi, J., Bergenstock, M., Shapses, S., Feyen, J. H., Notterman, D. A., and Partridge, N. C. (2007) *J. Biol. Chem.* **282,** 33086–33097
4. Billinghurst, R. C., Dahlberg, L., Ionescu, M., Reiner, A., Bourne, R., Rorabeck, C., Mitchell, P., Hambor, J., Diekmann, O., Tschesche, H., Chen, J., Van Wart, H., and Poole, A. R. (1997) *J. Clin. Invest.* **99,** 1534–1545
5. Andereya, S., Streich, N., Schmidt-Rohlfing, B., Mumme, T., Müller-Rath, R., and Schneider, U. (2006) *Rheumatol. Int.* **26,** 432–438
6. Ala-aho, R., Ahonen, M., George, S. J., Heikkilä, J., Grénman, R., Kallajoki, M., and Kähäri, V. M. (2004) *Oncogene* **23,** 5111–5123
7. Scott, D. K., Brakenhoff, K. D., Clohisy, J. C., Quinn, C. O., and Partridge, N. C. (1992) *Mol. Endocrinol.* **6,** 2153–2159
8. Tuckermann, J. P., Pittois, K., Partridge, N. C., Merregaert, J., and Angel, P. (2000) *J. Bone Miner. Res.* **15,** 1257–1265
9. Lanske, B., Divieti, P., Kovacs, C. S., Pirro, A., Landis, W. J., Krane, S. M., Bringhurst, F. R., and Kronenberg, H. M. (1998) *Endocrinology* **139,** 5194–5204
10. Uchida, M., Yamato, H., Nagai, Y., Yamagiwa, H., Hayami, T., Tokunaga, K., Endo, N., Suzuki, H., Obara, K., Fujieda, A., Murayama, H., and Fukumoto, S. (2001) *J. Bone Miner. Metab.* **19,** 207–212
11. Inada, M., Wang, Y., Byrne, M. H., Rahman, M. U., Miyaura, C., López-Otín, C., and Krane, S. M. (2004) *Proc. Natl. Acad. Sci. U.S.A.* **101,** 17192–17197
12. Stickens, D., Behonick, D. J., Ortega, N., Heyer, B., Hartenstein, B., Yu, Y., Fosang, A. J., Schorpp-Kistner, M., Angel, P., and Werb, Z. (2004) *Development* **131,** 5883–5895
13. Miao, D., He, B., Karaplis, A. C., and Goltzman, D. (2002) *J. Clin. Invest.* **109,** 1173–1182
14. Selvamurugan, N., Chou, W. Y., Pearman, A. T., Pulumati, M. R., and Partridge, N. C. (1998) *J. Biol. Chem.* **273,** 10647–10657
15. Winchester, S. K., Selvamurugan, N., D'Alonzo, R. C., and Partridge, N. C. (2000) *J. Biol. Chem.* **275,** 23310–23318
16. Ducy, P., Zhang, R., Geoffroy, V., Ridall, A. L., and Karsenty, G. (1997) *Cell* **89,** 747–754
17. Selvamurugan, N., Shimizu, E., Lee, M., Liu, T., Li, H., and Partridge, N. C. (2009) *FEBS Lett.* **583,** 1141–1146
18. Sierra, J., Villagra, A., Paredes, R., Cruzat, F., Gutierrez, S., Javed, A., Arriagada, G., Olate, J., Imschenetzky, M., Van Wijnen, A. J., Lian, J. B., Stein, G. S., Stein, J. L., and Montecino, M. (2003) *Mol. Cell. Biol.* **23,** 3339–3351
19. Komori, T., Yagi, H., Nomura, S., Yamaguchi, A., Sasaki, K., Deguchi, K., Shimizu, Y., Bronson, R. T., Gao, Y. H., Inada, M., Sato, M., Okamoto, R., Kitamura, Y., Yoshiki, S., and Kishimoto, T. (1997) *Cell* **89,** 755–764
20. Choi, J. Y., Pratap, J., Javed, A., Zaidi, S. K., Xing, L., Balint, E., Dalamangas, S., Boyce, B., van Wijnen, A. J., Lian, J. B., Stein, J. L., Jones, S. N., and Stein, G. S. (2001) *Proc. Natl. Acad. Sci. U.S.A.* **98,** 8650–8655
21. Jiménez, M. J., Balbín, M., López, J. M., Alvarez, J., Komori, T., and López-Otín, C. (1999) *Mol. Cell. Biol.* **19,** 4431–4442
22. Shimizu, E., Selvamurugan, N., Westendorf, J. J., Olson, E. N., and Partridge, N. C. (2010) *J. Biol. Chem.* **285,** 9616–9626
23. Boumah, C. E., Lee, M., Selvamurugan, N., Shimizu, E., and Partridge, N. C. (2009) *Mol. Endocrinol.* **23,** 1255–1263
24. Ogryzko, V. V., Schiltz, R. L., Russanova, V., Howard, B. H., and Nakatani, Y. (1996) *Cell* **87,** 953–959
25. Bannister, A. J., and Kouzarides, T. (1996) *Nature* **384,** 641–643
26. Sakaguchi, K., Herrera, J. E., Saito, S., Miki, T., Bustin, M., Vassilev, A., Anderson, C. W., and Appella, E. (1998) *Genes Dev.* **12,** 2831–2841
27. Jeon, E. J., Lee, K. Y., Choi, N. S., Lee, M. H., Kim, H. N., Jin, Y. H., Ryoo, H. M., Choi, J. Y., Yoshida, M., Nishino, N., Oh, B. C., Lee, K. S., Lee, Y. H., and Bae, S. C. (2006) *J. Biol. Chem.* **281,** 16502–16511
28. Puri, P. L., Sartorelli, V., Yang, X. J., Hamamori, Y., Ogryzko, V. V., Howard, B. H., Kedes, L., Wang, J. Y., Graessmann, A., Nakatani, Y., and Levrero, M. (1997) *Mol. Cell* **1,** 35–45
29. Lee, K., Brown, D., Ureña, P., Ardaillou, N., Ardaillou, R., Deeds, J., and Segre, G. V. (1996) *Am. J. Physiol.* **270,** F186–F191
30. Yang, X. J., Ogryzko, V. V., Nishikawa, J., Howard, B. H., and Nakatani, Y. (1996) *Nature* **382,** 319–324
31. Schiltz, R. L., Mizzen, C. A., Vassilev, A., Cook, R. G., Allis, C. D., and Nakatani, Y. (1999) *J. Biol. Chem.* **274,** 1189–1192
32. Santos-Rosa, H., Valls, E., Kouzarides, T., and Martínez-Balbás, M. (2003) *Nucleic Acids Res.* **31,** 4285–4292
33. Shalhoub, V., Conlon, D., Tassinari, M., Quinn, C., Partridge, N., Stein, G. S., and Lian, J. B. (1992) *J. Cell. Biochem.* **50,** 425–440
34. Caretti, G., Di Padova, M., Micales, B., Lyons, G. E., and Sartorelli, V. (2004) *Genes Dev.* **18,** 2627–2638
35. Chérasse, Y., Maurin, A. C., Chaveroux, C., Jousse, C., Carraro, V., Parry, L., Deval, C., Chambon, C., Fafournoux, P., and Bruhat, A. (2007) *Nucleic Acids Res.* **35,** 5954–5965
36. Deng, W. G., Zhu, Y., and Wu, K. K. (2004) *Blood* **103,** 2135–2142
37. Wallberg, A. E., Pedersen, K., Lendahl, U., and Roeder, R. G. (2002) *Mol. Cell. Biol.* **22,** 7812–7819
38. Tsai, L. N., Ku, T. K., Salib, N. K., and Crowe, D. L. (2008) *Mol. Cell. Biol.* **28,** 4240–4250
39. Korzus, E., Torchia, J., Rose, D. W., Xu, L., Kurokawa, R., McInerney, E. M., Mullen, T. M., Glass, C. K., and Rosenfeld, M. G. (1998) *Science* **279,** 703–707
40. Li, A., Xue, Y., Jin, C., Wang, M., and Yao, X. (2006) *Biochem. Biophys. Res. Commun.* **350,** 818–824
41. Selvamurugan, N., Pulumati, M. R., Tyson, D. R., and Partridge, N. C. (2000) *J. Biol. Chem.* **275,** 5037–5042
42. Blanco, J. C., Minucci, S., Lu, J., Yang, X. J., Walker, K. K., Chen, H., Evans, R. M., Nakatani, Y., and Ozato, K. (1998) *Genes Dev.* **12,** 1638–1651
43. Kuninger, D., Wright, A., and Rotwein, P. (2006) *Am. J. Physiol. Cell Physiol.* **291,** C699–C709
44. Xu, W., Edmondson, D. G., Evrard, Y. A., Wakamiya, M., Behringer, R. R., and Roth, S. Y. (2000) *Nat. Genet.* **26,** 229–232
45. Yamauchi, T., Yamauchi, J., Kuwata, T., Tamura, T., Yamashita, T., Bae, N., Westphal, H., Ozato, K., and Nakatani, Y. (2000) *Proc. Natl. Acad. Sci. U.S.A.* **97,** 11303–11306
46. Yao, T. P., Oh, S. P., Fuchs, M., Zhou, N. D., Ch'ng, L. E., Newsome, D., Bronson, R. T., Li, E., Livingston, D. M., and Eckner, R. (1998) *Cell* **93,** 361–372